Experimental investigation on hygrothermal performance of a bio-based wall made of cement mortar filled with date palm fibers

Nawal Chennouf, Boudjemaa Agoudjil, Tarek Alioua, Abderrahim Boudenne, Karim Benzarti

Experimental investigation on hygrothermal performance of a bio-based wall made of cement mortar filled with date palm fibers

Nawal Chennouf[1, 2], Boudjemaa Agoudjil[2*], Tarek Alioua[1, 2], Abderrahim Boudenne[1*], Karim Benzarti[3]

[1]*Université Paris Est Créteil Val de Marne, CERTES, 61 Av. du Général de Gaulle, 94010 Créteil Cedex, France ;*
[2]*Université Batna -1, LPEA, Les Allées 19 mai Route de Biskra Batna, Algeria;*
[3]*Université Paris-Est, Laboratoire NAVIER, UMR8205, IFSTTAR, F77447 Marne la Vallée, France ;*

Abstract:

In the present work, the hygrothermal behavior of a wall structure made of a novel biobased material, *i.e.* date palm fiber reinforced concrete was investigated. In this context, a specific setup was developed which allows simulating a bi-climatic environment with separate outdoor and indoor environments. This device made it possible to apply various scenarios of static / dynamic hygrothermal loading to the outer side of wall, involving variation/cycling of temperature (T) and /or relative humidity (RH). During these experiments, resulting variations of T and RH across the wall thickness were monitored with in-situ sensors. Outstanding thermo-hygric phenomena were highlighted, such as high coupling effect between heat and moisture transfers, resulting from evaporation-condensation and sorption-desorption processes. Besides, significant thermal and hygric inertia was observed through the Date Palme Concrete (DPC) wall. The response time of this DPC wall to temperature variations remains shorter than in the case of humidity variations. Even so, large damping effect is obtained compared to outdoor boundary conditions, which make this DPC wall a good candidate for mitigating overheating during summertime and reducing interstitial condensation as well.

Keywords

Hygrothermal behavior; Thermal inertia; Heat and moisture transfers; Biobased material; Date Palm Concrete

*__Corresponding authors__:

*Dr. Abderrahim Boudenne, email: boudenne@u-pec.fr

Université Paris-Est Créteil Val de Marne, (UPEC)/CERTES, 61 Av. du Général de Gaulle 94010 Créteil cedex, France.

*Pr. Boudjemaa Agoudjil, email: boudjemaa.agoudjil@univ-batna.dz

Université Batna 1, 1rue chahid Boukhlouf Mohamed El-hadi 05000 Batna, Algeria.

1 Introduction

World energy consumption has been growing rapidly in the construction sector, causing an increase in CO_2 emission of 43% over the last two decades [1]. These trends are closely related to the economic development and population growth, and they contribute to exhaust natural resource and to degrade the environment (ozone layer depletion, global warming, climate change, etc.). Therefore, current public policies are promoting the development of innovative technologies capable of improving energy efficiency, with specific interest in "green technologies" based on renewable resources, waste valorization or recycled materials [2].

In this context, the replacement of conventional building materials (concrete or hydraulic mortars) by bio-based materials with low thermal conductivity has emerged as an interesting solution for both upgrading the thermal performances and reducing the carbon footprint of buildings [3]. In addition, these bio-based materials generally exhibit hygroscopic behavior which enable them to absorb or release moisture, and hence, to reduce humidity variations of the indoor air [4]. Therefore, they are not only effective as thermal insulation materials, but also offer benefits in terms of comfort and health for the occupants.

Recently, several materials containing natural fibers have been introduced in construction [5]. Some of these include date palm wood, which presents a real potential for building applications around the world [6]. This component can be used as reinforcement in various matrices such as gypsum, polymers and concrete [7-9].

Mechanical and physical properties of Date Palm Concrete (DPC) including 15 wt. % of date palm fibers have been explored in different studies from the literature [7, 10, 11]. This bio-based material is a lightweight building material characterized by a compressive strength (Rc) of 2.64 MPa and a low thermal conductivity (k) of 0.14 $W.m^{-1}.K^{-1}$,which fulfils RILEM requirements for structural and insulating autoclaved aerated concretes (Rc>2.5 MPa, $k<0.75W.m^{-1}.K^{-1}$) [7]. Besides, this DPC material was found to exhibit a strong hygroscopic behavior [7], resulting in very good hygrothermal performances and excellent capacity of moisture regulation. Its porosity, water vapor diffusion resistance in the dry and humid states, sorption behavior, and moisture buffering value were also investigated in references [10] and [11].

Nevertheless, experimental evaluation of DPC performances at the material scale and under steady state conditions is not enough to fully validate the suitability of this building material. In actual service conditions, building structures are indeed subjected to dynamic weathering

conditions, and very different hygrothermal boundary conditions apply on the external side of the envelope and inside the building. For all these reasons, the present work will be focused on investigating the hygrothermal behavior of DPC at the wall scale and under bi-climatic conditions, considering different temperature-humidity scenarios.

Over the last 5 years, several studies from the literature explored the hygrothermal behavior of building materials at the wall scale. Some of them involved numerical approaches based on heat and mass transfer calculations [12,13], while others involved experimental approaches using climate chambers or onsite exposures [14,15]; these studies were carried out on either conventional or bio-based building materials [16].

Latif *et al*. [14] used a bi-climatic chamber to study the hygrothermal behavior of three different panels made of mineral wool, wood fibers, and a combination of wood fibers and hemp-lime [14,17]. Pavlík *et al.* investigated the hygrothermal performance of a designed insulation system under conditions corresponding to the winter climate in Middle Europe [18]. Hemp concrete was also studied at the wall scale in the literature, both experimentally and numerically [15,19,20]. The results obtained show a strong coupling between the heat and moisture transfer. Therefore, hemp concrete behaves as natural phase change material there by substantially dampens temperature variations in the wall [21]. Considering the high thermal insulation efficiency and the weak mechanical properties of straw, a load-bearing structure combining straw bales and wooden frames is of great interest. Douzan *et al*. [22] have compare the U-value of a straw bale wall to different walls used in civil field engineering. In parallel several in situ experimental studies have also been conducted to evaluate the hygric and thermal performance of wall panels or insulation materials [23-25].

The present work deals with the hygrothermal behavior of a bio-based wall made of concrete filled with wastes of Date Palm Fibers (DPF). Investigations were focused on checking the ability of this material to moderate the cyclic variations of both humidity and temperature. Heat and moisture coupling mechanisms in DPC were also studied. The study was carried out using a specific experimental setup that allows to apply separate hydrothermal conditions on each side of the wall (bi-climatic configuration), and considering five different scenarios for the outdoor boundary conditions. Distributions of temperature (*T*) and relative humidity (*RH*) across the wall thickness were continuously monitored during the tests, as well as T and RH values in the indoor environment. Results are discussed for the various loading scenarios.

2 Materials and methodology

2.1 Wall preparation

In accordance with previous studies, a formulation of concrete filled with 15*wt.* % of date palm fibers was selected for this work, as the resulting hardened material exhibits interesting thermo-physical, mechanical [5,6] and hygric properties with respect to building applications [7]. DPC can be classified among lightweight building materials, and its thermal conductivity (*k*) depends on both the formulation, density and water content. The value of *k* ranges from 0.14 in the dry state to 0.24 ($W.m^{-1}.K^{-1}$) in the wet state[11].

Like all bio-aggregate based materials, DPC is strongly hygroscopic and exhibits much higher water uptake than conventional building materials [11]. DPC is characterized by low density and high porosity, leading to excellent hygric properties and insulation capacity [7,10,11]. At low and high RH levels, the water vapor diffusion resistance of DPC is respectively equal to 6.31 and 5.57 [11]. In addition, when considering the adsorption /desorption behaviour, this DPC material shows excellent moisture buffering capacity and large hysteresis [11] according to the Nordtest project classification [25]. Values of DPC properties as well as the corresponding references are reported in Table 1.

In the framework of this study, a DPC wall of dimension 0.5 m×0.4 m×0.15 m (length × height × thickness) was fabricated. This bio-concrete formulation consisted of 62 wt.% cement (CEM II/B-LL32.5R CE NF), 23 wt.% sand (particle size 0-4 mm) and 15 wt. % DPF (mean diameter = 3 mm). A water to cement ratio W/C of 0.68 was chosen in accordance with previous works [10,11].

First, components were mixed at the dry state in order to obtain a homogeneous mixture. Water was then added gradually while mixing regularly, until obtaining a homogeneous fresh composite mix. At the next step, the mix was gradually casted layer by layer in a wooden mold; this operation was made with caution in order to avoid creation of air bubbles or empty spaces in the molded wall. Three weeks later, the hardened wall was removed from the mold. Finally, it was left to dry in the laboratory environment (at 50% RH and 20°C) for one year. During the drying process, temperature and relative humidity were measured periodically to check they remained constant.

Table 1: DPC properties

Property	Value	Reference	Property	Value	Reference
Dry density [kg/m^3]	954	[11]	Dry specific heat [J.kg^{-1}.K^{-1}]	1500	[7]
Dry thermal conductivity [W.m^{-1}.K^{-1}]	0.185	[11]	Porosity [-]	64	[11]
Vapor resistance factor (dry cup) [-]	6.310	[10]	Vapor resistance factor (wet cup) [-]	5.570	[10]
Water absorption coefficient [kg.m^{-2}s$^{-0.5}$]	0.165	[11]	Water content at free saturation [kg.m^{-3}]	429	[11]

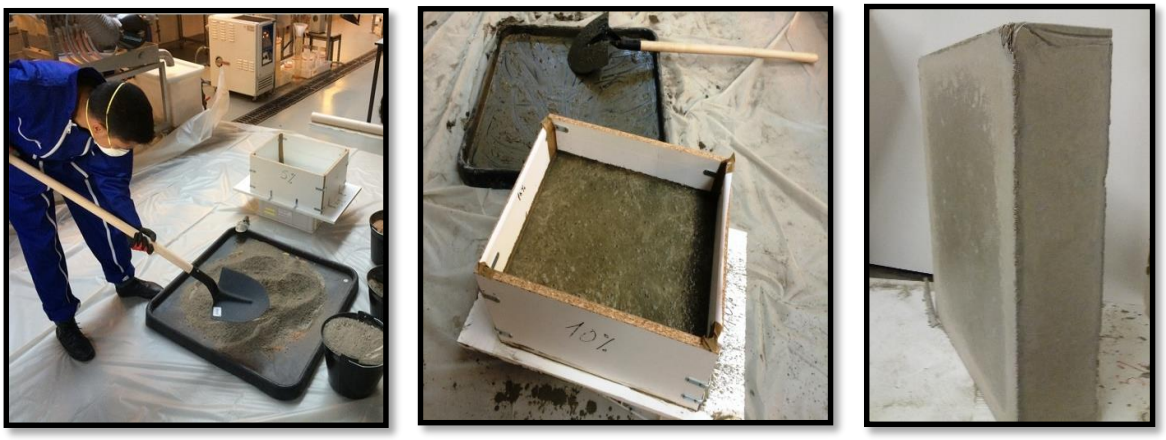

Figure1: Mixing of the material components and casting of the DPC wall.

2.2 Instrumentation

Measurements and monitoring of RH and T within the wall were performed with DKRF400 humidity/temperature sensors from Driesen + Kern, Germany (measurement range of RH: 0-100% with an accuracy of ±1.8 %, and measurement range of T: -40°C to +45°C with an accuracy of ± 0.5°C). Sensors have a diameter of 8 mm and a length of 100 mm, and can be easily inserted into the wall at different depth levels. Following the recommendation of Hedenblad *et al*. [21], our humidity/temperature sensors were inserted along the isothermal and iso-humidity lines. The probes were placed at three strategic locations, i.e., close to the inner and outer sides of the wall (respectively at abscissa x = 3 cm and x = 12.5 cm) and at the center of the wall (x = 7.5 cm), as shown in Figure 2. All sensors were connected to a data acquisition

module (model OM-DAQ-USB-2401 from Omega Engineering, USA), and this latter was plugged to a computer via USB port. This metrological chain can automatically collect data from the connected sensors with an acquisition step of 60 seconds, which allows a continuous monitoring of temperature and hygrometry at the various sensor locations.

2.3 Experimental Setup

The experimental device consists of a climatic chamber (Model HPP750 from Memmert, Germany) in order to simulate the dynamic outdoor climate conditions, and another passive cell to simulate the indoor climate conditions (Figure 2). The response of the wall subjected to this bi-climatic configuration (applications of cyclic or static variations of T and RH by the climatic chamber on the outer side of the wall, and fixed initial conditions of the passive cell on the inner side of the wall) allows evaluating the hygrothermal performances of the DPC wall.

The main objective is to evaluate the potential of the DPC wall for the mitigation of humidity and temperature variations. This experimental configuration is inspired from the works of Latif *et al*., Ferroukhi *et al*. and Rahim *et al*. [17, 21, 28]. It is developed to simulate the application of weathering stresses on the outer side of the wall, while the temperature and humidity of the indoor air is not controlled (*i.e*., this is typically representative of a building which has no air conditioning system). Major advantages of the proposed setup are its low cost and reduced volume, compared to commercial bi-climatic chambers which are both very expensive and bulky. Of course, testing possibilities are more limited in return, excluding the situations where the indoor environment is fully controlled.

The HPP750 climatic chamber can operate in the temperature range 0 -70 °C and also in the humidity range 10 - 90 % RH thanks to a dry air purge system that allows quasi instantaneous changes from high to low RH levels. The passive cell is made of 5 expanded polystyrene panels (U= 0.5 [$W.m^{-2}. K^{-1}$]) connected to the wall and is also wrapped by a thick glass wool layer (U= 0.2 [$W.m^{-2}. K^{-1}$]) protected by a thin external plastic film, which acts both as thermal insulation and a waterproof barrier.

Prior to any experiment, a conditioning phase at 50% RH and 23°C is applied by the climatic chamber, until the equilibrium is reached in the passive cell. Then, for the test program, specific dynamic boundary conditions can be applied by the climatic chamber, while the indoor conditions of the passive cell are left uncontrolled. In these conditions, thermal and hygric transfers between the chamber and the passive cell are thus governed by the DPC wall.

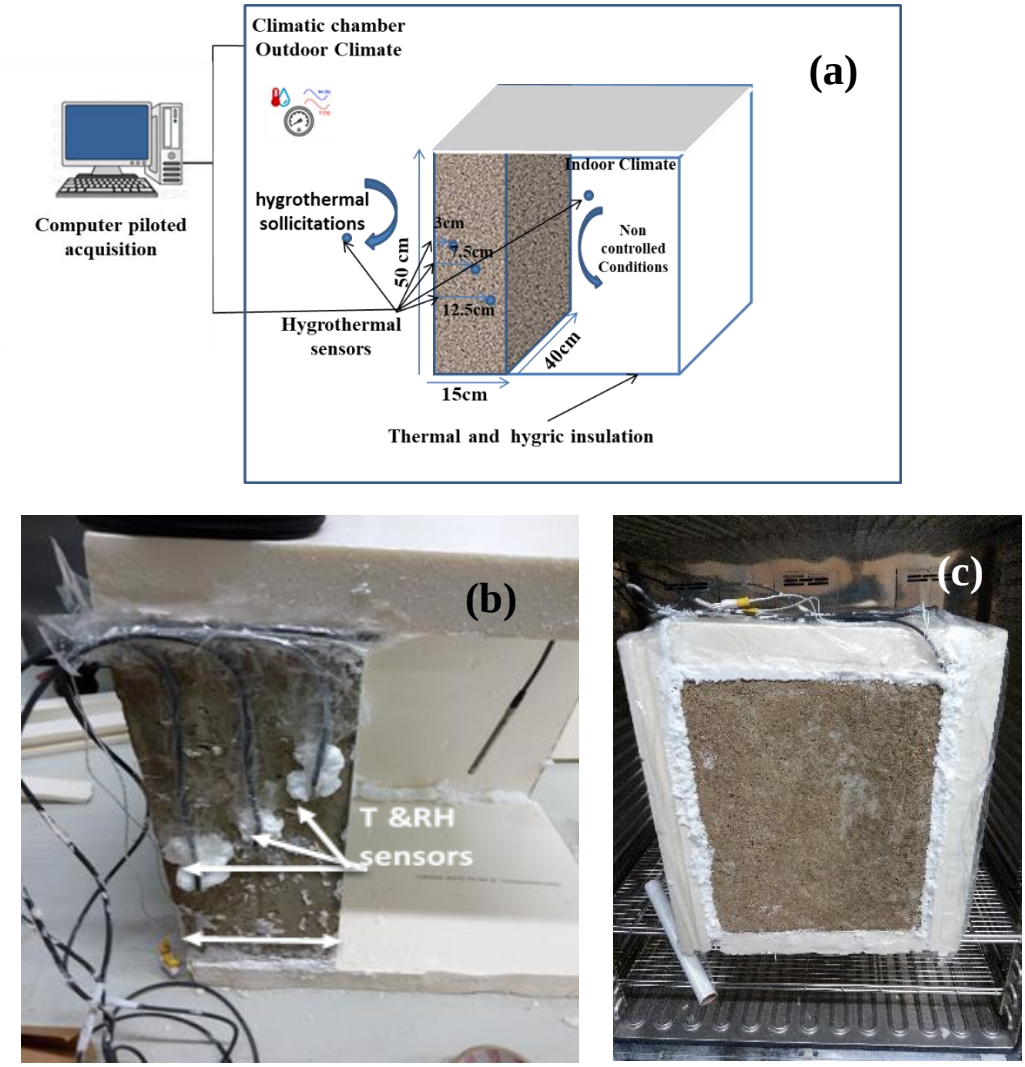

Figure 2: a) Overall experimental setup, b) humidity/temperature sensors after installation in the wall cross-section, c) Picture of the wall connected to the passive cell (indoor environment) and installed inside the HPP750 climatic chamber (outdoor environment).

2.4 Application of Boundary Conditions

Hygrothermal performance of a building envelope is dictated by the capacity of the system to mitigate heat and moisture fluctuations of the indoor environment, which can be influenced by both outdoor dynamic boundary conditions and by human activity inside the building.

In the present study, only the influence of external boundary conditions is considered. As stated in section 2.3, initial boundary conditions of the indoor environment (at the inner side of the

wall) were adjusted to 23°C and 50% RH before starting any experiment and they were not controlled afterwards.

Table 2 summarizes the five programmed scenarios on the Memmert HPP750 climatic chamber to simulate different dynamic boundary conditions applied to the outer side of the wall. As far as we know, there are no at this time a standard scenarios or technical specifications in order to study at the wall scale the performance of the biobased building materials. In this work, the applied scenarios are chosen on the basis of previous works as well as the objectives set [17,22,23,25]. Scenario 1 consists in periodic RH cycling at constant temperature (adsorption/desorption phases with step changes between 75-33% RH), while scenarios 2 and 3 simulate daily temperature variations during summertime (hot/cold periods of 12 hours with step changes between 40-18°C) at constant humidity level (50% RH) or without RH control, respectively. Scenario 4 involves an initial temperature increment from 23° to 40°C followed by a prolonged period at 40°C, while RH is maintained at 50%. Finally, scenario 5 combines both T and RH cycling, with step changes from a boundary condition at 40°C / 33% RH to another condition at 18°C / 75% RH. Periods of the cycles are also mentioned in Table 2 when relevant.

As the wall with the passive cell occupy an important part of the climatic chamber, there is a risk that the system (wall + passive cell) affects the dynamic response of the climatic chamber as well as the homogenization of the set points (outdoor conditions). For this reason, preliminary tests were carried out to check if the performance (in terms of temperature / humidity control) of the Memmert climatic chamber in presence of the passive cell allows a proper application of the dynamic conditions for the various scenarios. In this regard, measurements of T and RH were performed inside of the climatic chamber using a DKRF400 sensor, and then compared to the programmed values. This comparison is illustrated in Figure 3 where the T set points of scenarios 3, 4, 5 are and only presented Figure 3b.

Figure 3 shows that the climatic chamber follows very well the dynamic conditions imposed in the different scenarios (step changes in T / RH), thanks to low inertia and effective temperature/moisture control of the apparatus. Nevertheless, experimental curves show small fluctuations around the set temperature/moisture points due to the on/off regulation of the control system. Moreover, RH fluctuations presented in figure 3.c were unexpected since outdoor RH level is set constant at 50% in scenario 2; such a phenomenon is caused by moisture

released or absorbed by the wall during T cycling and will be discussed at a later stage in this paper.

Table 2: Boundary conditions applied to the outer side of the DPC wall (values in brackets correspond to the initial boundary conditions at the beginning of the experiment, *i.e.*, 23°C and 50% RH)

	T[°C]	**RH [%]**	**Cycle period** (for the varying parameter, if relevant)
Scenario 1	23	(50) →75→33	18 days (9 days at 75% RH, 9 days at 33% RH)
Scenario 2	(23)→ 40 →18	50	24 hours (12 h at 40°C, 12 h at 18°C)×5
Scenario 3	(23) → 40 → 18	Not controlled	24 hours (12 h at 40°C, 12 h at 18°C)×11
Scenario 4	(23) → 40	50	No cycle (initial step change of T, followed by prolonged exposure at 40°C and 50% RH for 6 days)
Scenario 5	(23) → 40 → 18	(50) →33→75	24 hours (12h at 40°C and 33% RH, 12 h at 18°C and 75% RH)×11

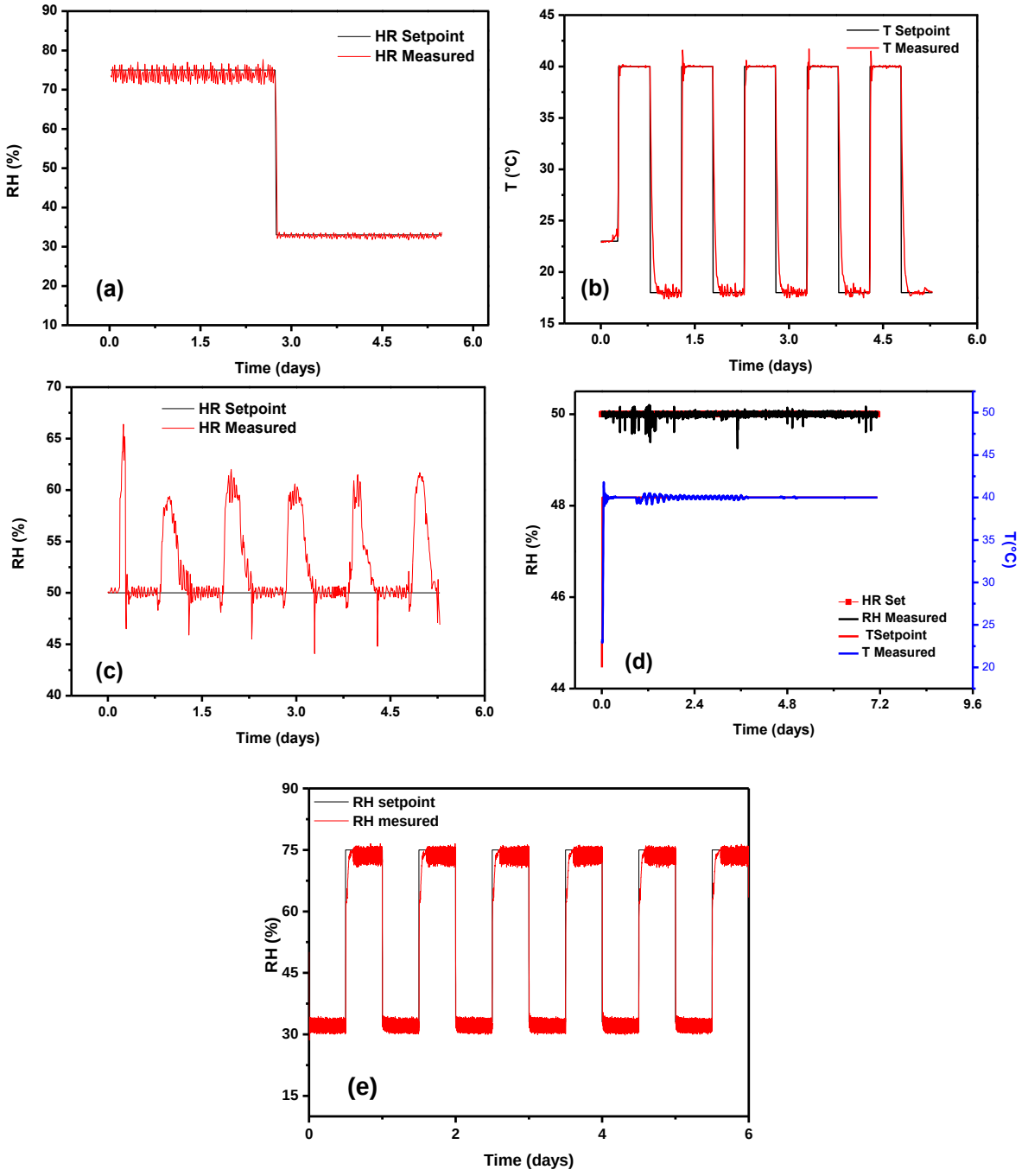

Figure 3: Response of the Memmert HPP750 climatic chamber to the boundary conditions: (a) boundary conditions of experiment 1, (b), (c) boundary conditions of experiment 2, (d) boundary conditions of experiment 4 and (e) RH boundary conditions of experiment 5.

3 Results and discussions

3.1 Experimental response of the DPC wall to humidity variations

An isothermal test was performed according to scenario 1 (see Table 1 and Figure 3.a). In a preliminary stage, the DPC wall was conditioned at 23°C and 50% RH until stabilization of the overall system. Then, the test started, and the outer side of the wall was subjected to a step RH change from 50 to 75%, while the temperature was kept constant at 23°C; these "outdoor" conditions were maintained for 9 days. Finally, RH at the outer wall was changed from 75% to 33% and maintained for another period of 9 days under constant temperature.

In this configuration, vapor transport occurred across the wall thickness, from the outdoor to the indoor of the DPC wall. The vapor pressure (p_v) can be calculated from the temperature T (in °C) and the relative humidity RH (in %) as follows [24]:

$$p_v = RH \times 100 \times Exp\left(18.986 - \frac{4052}{235.89+T}\right) \quad (1)$$

The outdoor water vapor pressure is 2400 Pa in the absorption phase (domain at 75% RH) and 296 Pa in desorption phase (domain at 33% RH), while the indoor water vapor pressure is 1400 Pa (at 50% RH), as calculated using Equation 1. Spatial variation of the vapor pressure across the wall thickness is correlated to RH variation, which can be assessed from sensor measurements.

Therefore, this experimental protocol allows evaluating the moisture buffering potential of the DPC wall under isothermal conditions.

Figure 4 presents RH variations as a function of time in the outdoor environment and at various depths within the tested DPC wall. At the beginning of the experiment, a step variation of RH from 50 to 75% is applied to the outdoor environment, while indoor RH level is fixed at 50%. Consequently, a vapor transfer takes place through the wall, which explains the observed RH increase across the wall thickness during the 9 days sorption phase.
However, the curves of Figure 4 show that kinetics of RH rise within the DPC wall is significantly higher at a depth of 3 cm than at depths of 7.5 and 12.5 cm. Consequently, after 9 days, values of RH are respectively 70, 65 and 64% at these depths. A similar trend is observed during the desorption phase, as RH decreases more rapidly at the location close to the outer side of the wall, compared to the two other locations at 7.5 and 12.5 cm away from this outer side.

RH variation shows high gradient near the outdoor side of the wall, while variations at 7.5 cm and 12.5 cm depths tend to be more linear with time. This is probably due to slow vapor diffusion process through the wall related to the acceptable water vapor resistance factor of DPC [7]. These results reflect the excellent moisture buffer capacity and the hygric inertia of DPC at the wall scale.

Besides, the indoor RH shows slightly higher values compared to RH obtained at 12.5 cm depth, which may result from a minor moisture infiltration taking place at the junction between the wall and the passive cell.

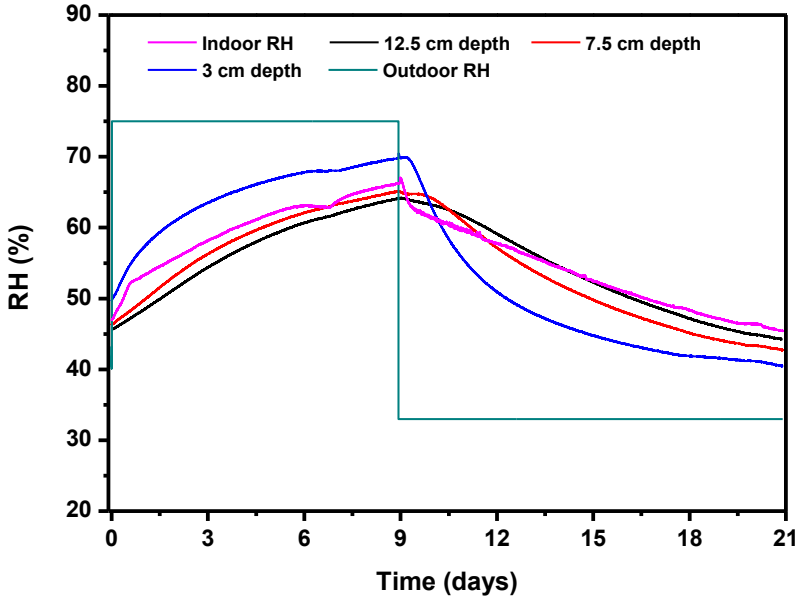

Figure 4: Variations of RH versus time at various depths of the DPC wall subjected to an adsorption / desorption scheme (scenario 1). The boundary condition imposed at the outer side of the wall is also displayed (outdoor RH), as well as the variation of indoor RH.

Figure 5 depicts the evolutions of temperature over time at the different sensor locations within the DPC wall during scenario 1. It is interesting to note that there is a sharp increase in T of about 1°C inside the wall at the beginning of the experiment, although the outdoor temperature remains constant at 23°C. This "*exothermic*" phenomenon occurs as outdoor RH is suddenly raised from 50 to 75%, and results from coupling effects between heat and mass transfers. Following this initial rise, temperature stabilizes around 24°C during the overall sorption phase.

Furthermore, as the desorption phase starts on the 9th day, the step variation of the outdoor RH from 75 to 33% is accompanied by a sharp drop of the wall temperature which returns close to the outdoor temperature of 23°C.

These results are in agreement with those obtained by Rahim *et al*., Aït Oumeziane *et al.* and Colinart *et al.* [23,25,26]. According to these authors, condensation takes place in the wall during adsorption phase; as it is an exothermic physical process, it leads to the observed T increase. On the opposite, evaporation occurs during desorption phase and is an endothermic phenomenon leading to a decrease in T. A small increase of T is observed in the passive cell air; the volume of the passive cell is considerably smaller than the climatic chamber, for this raison the interior air was influenced by the increase of wall T.

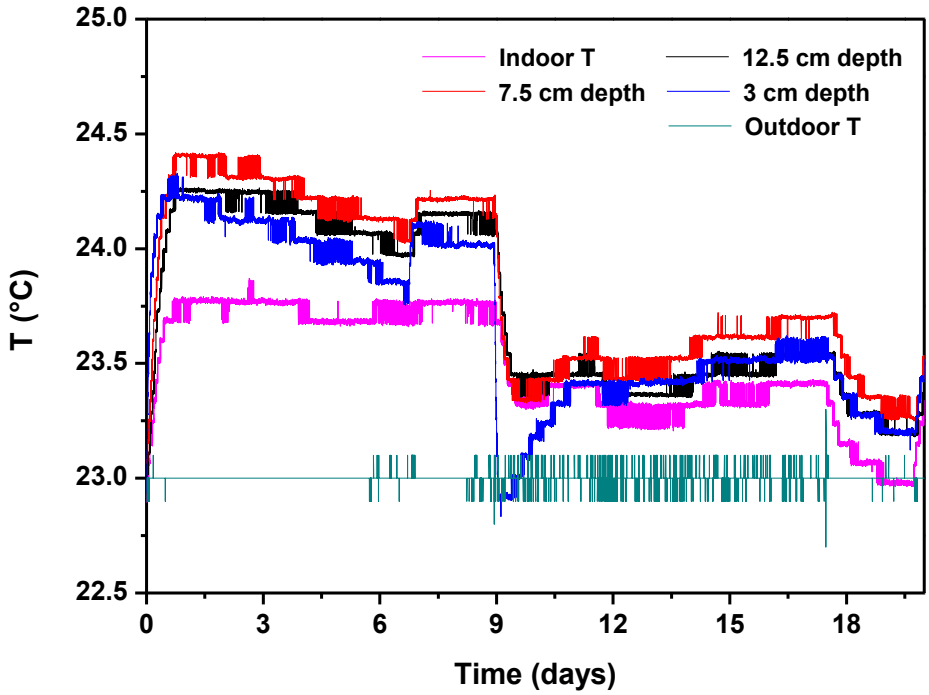

Figure 5: Evolution of temperature versus time at various depths of the DPC wall subjected to an adsorption / desorption scheme (scenario 1). Actual temperatures of the outdoor and indoor environments are also displayed.

3.2 Experimental response of the DPC wall to temperature variations

3.2.1 *Temperature cycling at constant humidity (RH = 50%).*

The thermal behavior of the DPC wall was also investigated. In order to evaluate the hygrothermal response of the wall to daily variation of temperature in summertime, a dynamic

test was carried out by varying the outdoor temperature in the range of 18-40°C at a constant RH level of 50% (scenario 2).

Prior to testing, the DPC wall was conditioned at 23°C and 50% RH for one week. Then, the outer side of the DPC wall was exposed to periodic variations of T, as detailed in Table 1 and Figure 3.b: initial step increases up to 40°C and sustained exposure at 40°C for 12 hours, followed by step decrease to 18°C and sustained exposure at 18°C for 12 hours. This cycle was repeated five times in order to simulate a 5 days exposure and evaluate the thermal inertia of this new biobased wall.

Figure 6 presents the evolutions of temperature over time at different depths of the DPC wall, as monitored by the sensors installed at 3, 7.5 and 12.5 cm away from the outer side. Compared to results of the previous section, it can be noticed that the thermal response of the DPC wall is much faster than the hygric response.

Besides, during the heating period at 40°C, the highest temperature measured in the wall (about 34°C) is obtained at the depth of 3 cm, while temperatures recorded at depths of 7.5 and 12.5 cm do not exceed 32.5°C and 33°C, respectively.

In contrast, during the cooling period, the temperature measured at 3 cm depth decreases and reaches the value of the outdoor set point (*i.e.*, 18°C), whereas temperatures recorded at depths of 7.5 cm and 12.5 cm show more limited reduction down to 20.5°C.

Temperature at center of the wall is significantly mitigated compared to the outdoor set point, both during heating and cooling phases. From these data, the damping amplitude "Dp_{12h}" (difference between the heating set temperature values (40°C) and the ones recorded in the middle of the wall after 12 h) is equals to 7.5°C. These results show that DPC wall can dampen effectively the outdoor climate conditions, in particularly during the summer period where the temperature can reach 40°C or more.

Moreover, it is clear that in the configuration of scenario 2, a vapor pressure gradient exists between the wall and the outdoor environment. The vapor pressure (p_v) can be calculated from the temperature T (in °C) and the relative humidity RH (in %) using Equation 1.

Generally, capillary condensation occurs in smaller pores, and part of water molecules contained in larger pores is thus released in the porous structure (at this point, instantaneous DPC moisture content is supposed to be constant).

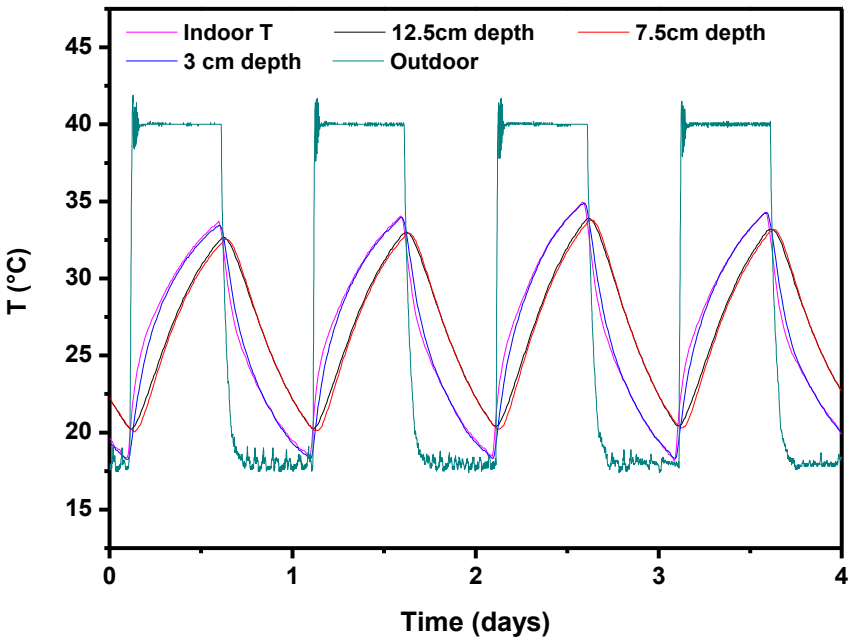

Figure 6: Thermal response of the DPC wall to temperature cycling according to scenario 2. Variations of the outdoor and indoor temperatures are also displayed.

Figures 7 (a) and (b) display respectively RH and vapor pressure variations at several depths within the DPC wall, and in the outdoor/indoor environments as well. It is found that the vapor pressure increases during heating phases, while it decreases during cooling periods. In the second part of each cycle, the set point decrease from 40°C to 18°C at a constant RH value (50%). This temperature drop is accompanied by both decrease of the relative humidity and the vapor pressure in the wall which is associated to the heat and mass transfer coupling phenomena. These features highlight the strong coupling between heat and moisture transfers across the wall. In addition, we notice that the amplitude of relative humidity cycles begins to increase slightly from the second cycle. This can be interpreted by the hygric inertia of the wall; where at each cycle, the DPC wall stores a certain quantity of moisture.

Moreover, as already stated in section 2.4., Figure 7 (a) shows that RH in the climatic chamber (outdoor RH) and in the passive cell (indoor RH) increase sharply during the step T decrease (at the beginning of the cooling period), due to the moisture released by the DPC wall. The moisture level then remains over the set point for few hours until the regulation system of the climatic chamber takes the control back and reduces the level down to 50% RH.

Nevertheless, the indoor temperature and relative humidity profiles are influenced mainly by the fluxes that cross the wall, and probably also by the heat and moisture infiltration from the lateral surface of DPC wall, as the insulation is not perfect.

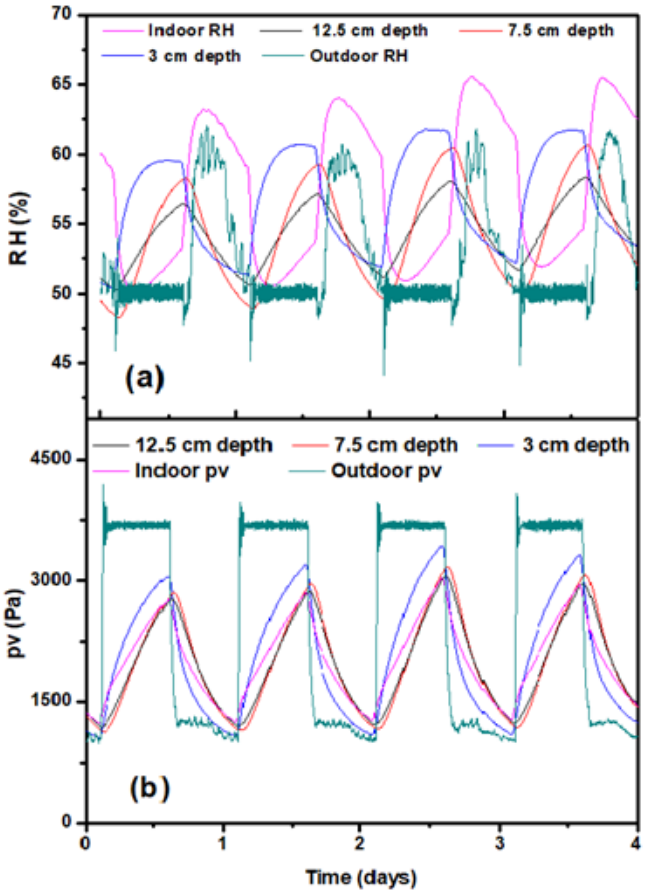

Figure 7: Variations over time of (a) the experimental RH and (b) the vapor pressure p_v derived from Equation 1, at depths of 3, 7.5 and 12.5 cm within the DPC wall subjected to temperature cycling and constant RH (scenario 2).

3.2.2 *Temperature cycling without RH control*

The response of the DPC wall to thermal cycling was also investigated in the case where outdoor RH is initially set at 50% and not controlled afterward during the test (scenario 3). The purpose was to explore further the coupling effects between temperature and moisture transfers.

Temperature and RH variations monitored at different depths of the DPC wall during this experiment are shown in Figure 8.

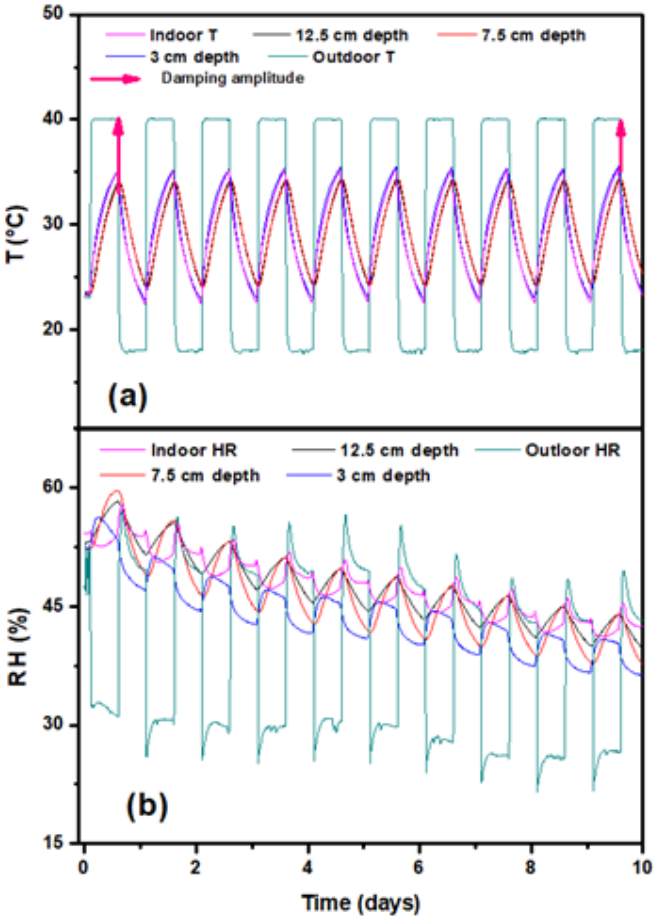

Figure 8: Variations over time of (a) Temperature and (b) Relative Humidity measured at different depths of the DPC wall subjected to temperature cycling without RH control (scenario 3). T and RH variations measured in the outdoor/indoor environments are also displayed.

First, it is found that temperature variations across the wall thickness (Figure 8.a) are almost similar to those obtained previously at constant RH level (Figure 6). One can only notice a small difference in the damping amplitude: this latter was about 7.5°C in the constant RH configuration, whereas it is slightly lower in the uncontrolled RH configuration and tends to reduce over the repeated cycles (6°C at the beginning of the test and 4.5°C after 10 days).

Likewise, the application of several thermal cycles in this test tends to reduce progressively the RH level within the DPC wall, as shown in Figure 8. In fact, each cycle involves local

evaporation/condensation phenomena in the wall and repeated cycles cause a global decrease in RH within the wall, which can be as high as 10% after 10 days.

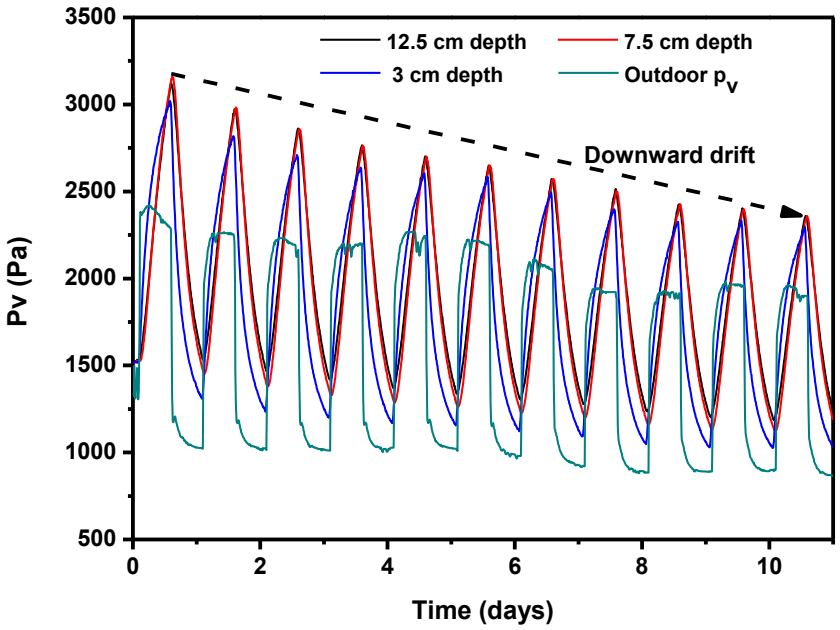

Figure 9: Variations over time of the vapor pressure at different depths of the DPC wall subjected to temperature cycling without RH control (scenario 3).

Figure 9 displays the variations of the vapor pressure (determined from Equation 1) in the wall, when applying the boundary conditions of scenario 3. The vapor pressure reflects the water content of the wall, and both are significantly affected by the repeated thermal cycles.

The results obtained in the present scenario are in agreement with those previously observed in scenario 2, as the vapor pressure profile follows the temperature cycles. In fact, the wall initially contains a certain amount of water vapor and, due to the evaporation phenomenon during heating phase, the vapor pressure increases in the wall. Furthermore, a progressive decrease in the maximum vapor pressure of the wall is observed over the repeated cycles (downward drift in Figure 9). This feature highlights a progressive drying of the wall during the test, in accordance with the variation of RH recorded across the wall thickness in Figure 8.b.

3.2.3 *Long heating period at constant humidity level (RH=50%).*

Scenario 4 consisted in applying a temperature gradient between the two sides of the wall, while maintaining outdoor RH constant at 50% (see Table 2).

Prior to testing, the DPC wall was conditioned at 23°C and 50%RH for 15 days. Then, a step variation of temperature from 23°C to 40°C was applied to the outer side of the wall at the beginning of the test and the outdoor temperature of 40°C was maintained for 6 days.

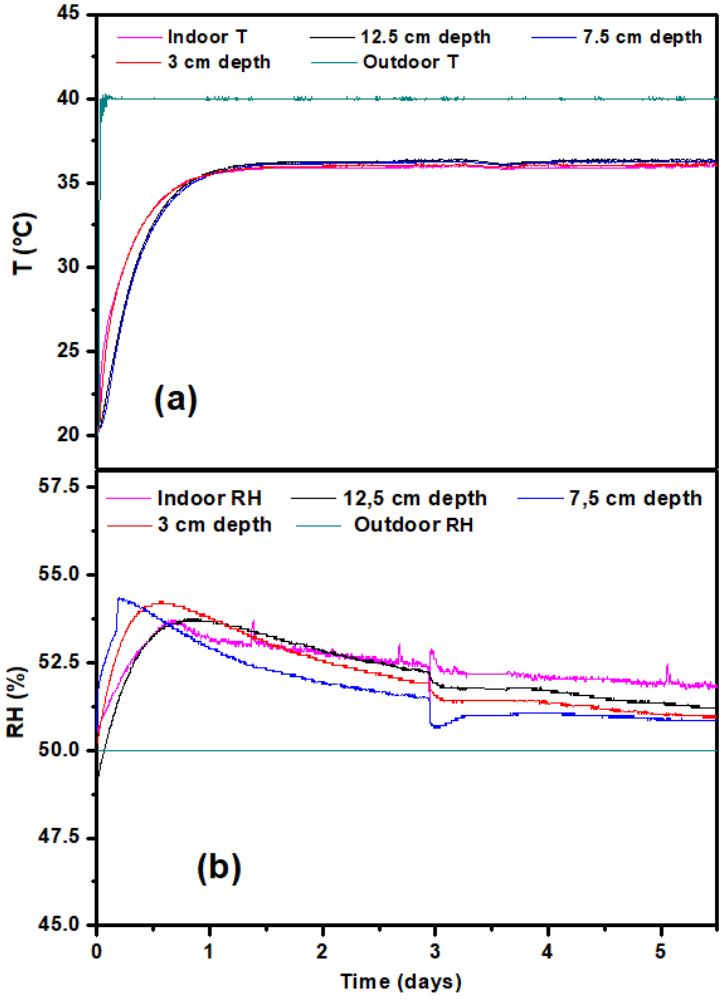

Figure 10: Evolution over time of (a) the temperature and (b) RH measured at different depths of the PDC wall subjected to prolonged exposure at 40°C under constant RH level (scenario 4). Boundary conditions in the outdoor environment are also displayed, as well as conditions measured in the indoor environment.

Figure 10 shows the variations of temperature and relative humidity within the DPC wall when applying boundary conditions of scenario 4.

From the results presented in Figure 10.a, it is found that temperature inside the wall increases from the beginning of the test and reaches a steady state at 36°C whatever the considered depth, and despite the significantly higher value of the outdoor temperature (40°C). Besides, this steady state is reached more quickly for the location close to the outer side of the wall (*i.e*, at a depth of 3 cm) compared to the 2 other locations. The difference between the equilibrium temperature in the wall and the outdoor temperature relates to the thermophysical properties of the DPC materials, *i.e.* high heat capacity and low thermal conductivity [14]
In addition, Figure 10.b shows that the prolonged heating phase also influences the hygric behavior of the DPC wall. Indeed, following the initial step variation of temperature, an increase in RH is observed within the wall until a steady state is reached, with kinetics depending on the distance to the outer side of the wall. Such an increase in RH is due to an evaporation phenomenon during heating phase.

3.2.4 *Simultaneous cyclic changes in temperature and humidity*

The main purpose of in this section is to evaluate the response of the DPC wall to combined thermal and moisture cycles representative of daily variations in summer conditions. In this line, dynamic outdoor boundary conditions were applied according to scenario 5 (cf. Table 1): after a preliminary conditioning of the system at 23°C and 50% RH, the test started by step variations of outdoor T and RH to 40°C and 33% respectively, and these conditions were maintained for 12h. Then, step variations were applied to reach T=18°C and RH=75% in the outdoor environment, and these parameters were kept constant for another 12 hours before repeating the cycle.

Variations of T and RH monitored over a period of 12 days at various depths of the wall are reported in Figures 12 and 13, respectively.
Here again, the thermal response of the wall exhibits large damping "Dp_{12h}" compared to boundary conditions, thanks to the low thermal conductivity of the DPC material. This feature is of major interest for mitigating outdoor temperature variations and avoiding overheating of the indoor environment during summertime.

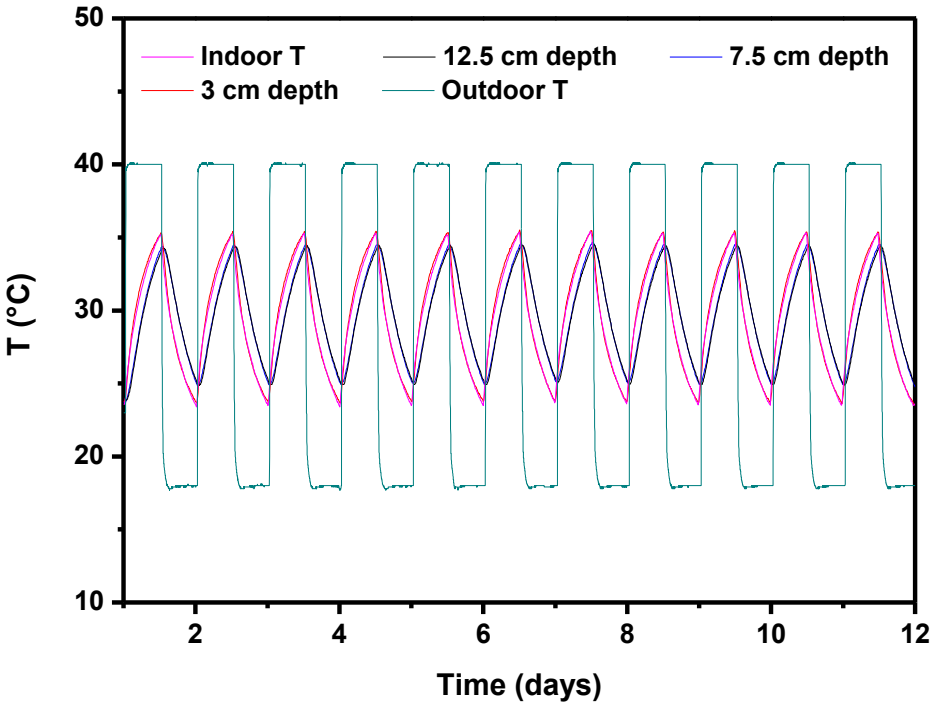

Figure 11: Thermal response of the DPC wall to combined temperature and moisture cycling according to scenario 5. Variations of the outdoor/indoor temperatures are also displayed.

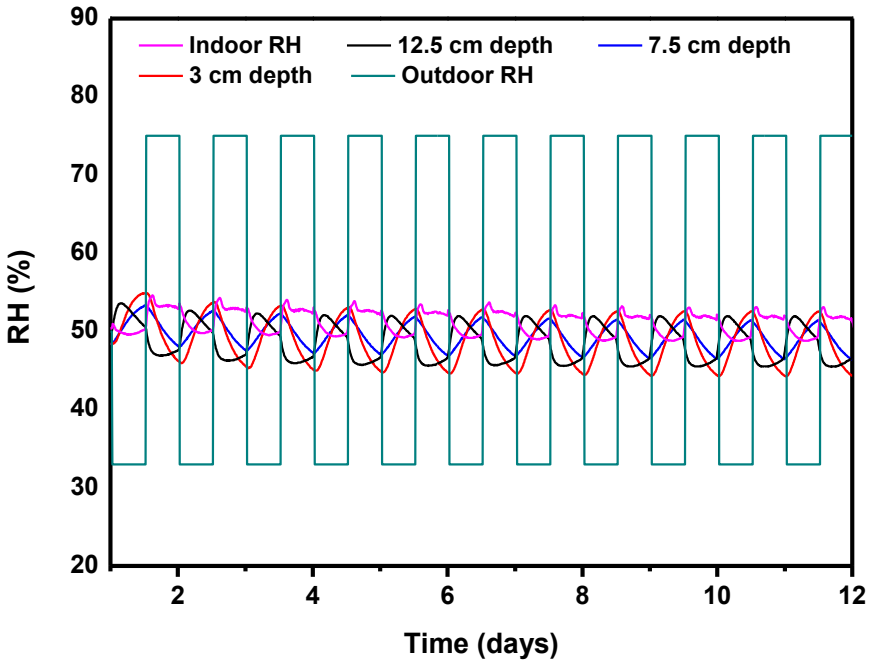

Figure 12: Variations over time of RH measured at different depths of the DPC wall subjected to combined temperature / moisture cycling (scenario 5). RH conditions in the outdoor/indoor environments are also displayed.

Furthermore, Figure 12 highlights that the DPC wall is only little affected by RH variation of the outdoor environments, as RH fluctuations remain very limited at all depths within the wall. These results are in accordance with those obtained by Chennouf *et al.*[10], who found a penetration depth less than 3.5 cm in the case of RH cycling according to the Nordtest protocol (cycle periods of 24 hours, as in the present case). Nevertheless, it must be underlined that this situation is different from that considered in scenario 1 with long periods of adsorption/desorption, where the wall was more deeply affected (Cf. section 3.1).

One can note that RH fluctuations in the indoor environment are also very limited, which highlights the capacity of the DPC wall to ensure the comfort of the inhabitants of a building.

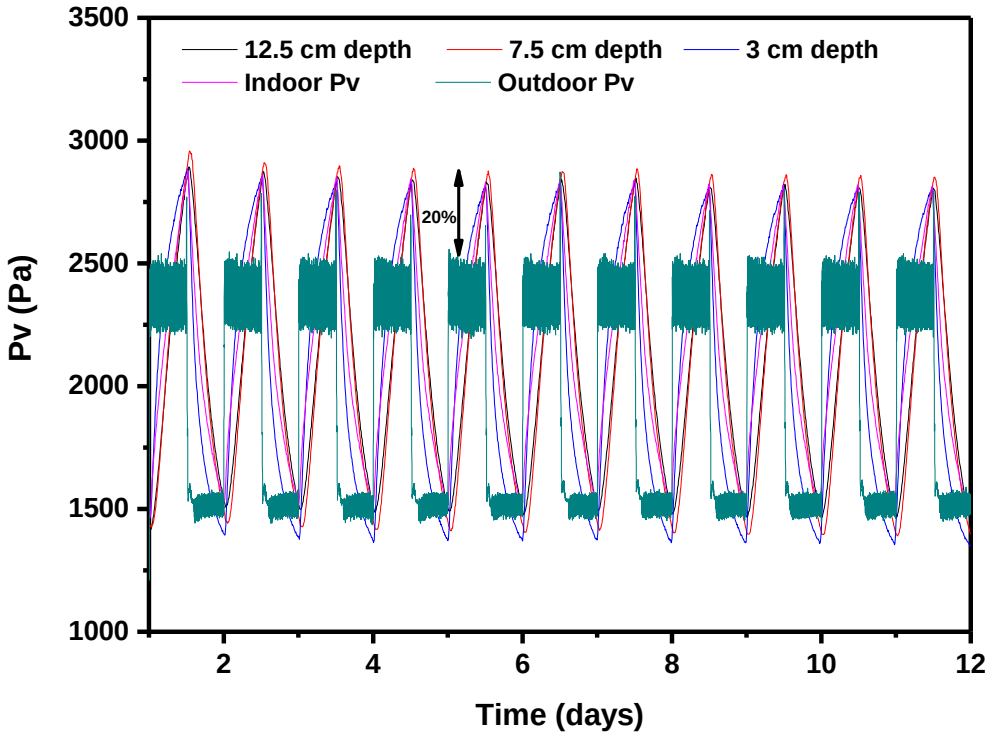

Figure 13: Variations over time of the vapor pressure at different depths of the DPC wall subjected to combined temperature / moisture cycling (scenario 5).

Figure 13 presents the variations of the vapor pressure p_v at different depths of the DPC wall over the repeated cycles of scenario 5. It can be noticed that values of p_v are much higher in the wall than in the outdoor environment during heating phase, while they are slightly lower during

cooling phase. The applied temperature cycles induce evaporation/condensation phenomena which correspond to the heating/cooling phases respectively. In the middle of the wall (at 7.5 cm depth), one can notice a 20% increase of p_v that seems independent of boundary conditions but probably related to vapor diffusion phenomena induced by heat transfer. The same observations were reported by Collet *et al*.[24], who highlighted an additional heat exchange due to adsorption-desorption phenomena.

From the results obtained in this last scenario, it is first found that the vapor pressure is more influenced by the temperature variation than by RH variations. Secondly, the DPC wall shows excellent hygric inertia which is only little influenced by external RH variations; consequently, the heat resulting from absorption/desorption phenomena is almost absent.

4 CONCLUSION

In the present work, the hygrothermal behavior of a new biobased material made of mortar filled with 15 wt.% date palm fibers was investigated at the wall scale. A simple bi-climatic setup was designed to apply steady or dynamic boundary conditions at the outer side of the wall, while the indoor environment was set at 23°C and 50% RH at the initial time and left uncontrolled during the experiments. For all configurations, hygrothermal response of the DPC wall was monitored thanks to temperature/moisture sensors installed at various depths across the wall thickness.

Results showed that this biobased material presents interesting hygric performance thanks to the Date Palm Fibers, which can contribute to mitigate variations of relative humidity. Likewise, DPC demonstrates good capacity for retaining / releasing heat in response to outdoor temperature excitation. Furthermore, as the DPC wall contributes to attenuate and dampen temperature variations, it offers an effective and ecological solution to reduce overheating during summertime. Besides, DPC exhibits very good hygrothermal performances, which makes this material suitable for thermal insulation and hygric regulation inside the buildings. Interaction between heat and mass transfers was also investigated in this work, and results highlighted very significant coupling effects between these two processes. In particular, a high influence of heat transfer on the hygric behavior of the DPC wall was revealed, which involves condensation / evaporation phenomena taking place in the microporous structure.

Several aspects of heat / moisture transfers were not tackled in this study, such as edge effects and evolution of the total moisture content of the wall in terms of gravimetric measurement. These issues should be addressed in future researches.

ACKNOWLEDGMENTS

Authors wish to acknowledge financial support of PHC TASSILI Project 16MDU976.

Reference

[1] L. Pérez-Lombard, J. Ortiz, and C. Pout, "A review on buildings energy consumption information," *Energy and buildings*, vol. 40, pp. 394-398, 2008.

[2] U. T. Haverinen-Shaughnessy, Mika Alm, Sari Putus, Tuula Nevalainen, Aino, "Personal and microenvironmental concentrations of particles and microbial aerosol in relation to health symptoms among teachers," *Journal of Exposure Science and Environmental Epidemiology*, vol. 17, pp. 182, 2007.

[3] F. Pittau, F. Krause, G. Lumia, and G. Habert, "Fast-growing bio-based materials as an opportunity for storing carbon in exterior walls," *Building and Environment*, vol. 129, pp. 117-129, 2018.

[4] A. T. Le, C. Maalouf, T. H. Mai, E. Wurtz, and F. Collet, "Transient hygrothermal behaviour of a hemp concrete building envelope," *Energy and buildings*, vol. 42, pp. 1797-1806, 2010.

[5] O. Faruk, A. K. Bledzki, H.-P. Fink, and M. Sain, "Biocomposites reinforced with natural fibers: 2000-2010," *Progress in polymer science*, vol. 37, pp. 1552-1596, 2012.

[6] B. Agoudjil, A. Benchabane, A. Boudenne, L. Ibos, and M. Fois, "Renewable materials to reduce building heat loss: Characterization of date palm wood," *Energy and buildings*, vol. 43, pp. 491-497, 2011.

[7] N. Benmansour, B. Agoudjil, A. Gherabli, A. Kareche, and A. Boudenne, "Thermal and mechanical performance of natural mortar reinforced with date palm fibers for use as insulating materials in building," *Energy and Buildings*, vol. 81, pp. 98-104, 2014.

[8] M. Chikhi, B. Agoudjil, A. Boudenne, and A. Gherabli, "Experimental investigation of new biocomposite with low cost for thermal insulation," *Energy and Buildings*, vol. 66, pp. 267-273, 2013.

[9] M. Haddadi, B. Agoudjil, N. Benmansour, A. Boudenne, and B. Garnier, "Experimental and modeling study of effective thermal conductivity of polymer filled with date palm fibers," *Polymer Composites*, vol. 38, pp. 1712-1719, 2017.

[10] N. Chennouf, B. Agoudjil, A. Boudenne, K. Benzarti, and F. Bouras, "Hygrothermal characterization of a new bio-based construction material: Concrete reinforced with date palm fibers," *Construction and Building Materials*, vol. 192, pp. 348-356, 2018.

[11] B. Haba, B. Agoudjil, A. Boudenne, and K. Benzarti, "Hygric properties and thermal conductivity of a new insulation material for building based on date palm concrete," *Construction and Building Materials*, vol. 154, pp. 963-971, 2017.

[12] A. Evrard and A. De Herde, "Hygrothermal performance of lime-hemp wall assemblies," *Journal of building physics*, vol. 34, pp. 5-25, 2010.

[13] M. Rahim, A. T. Le, O. Douzane, G. Promis, and T. Langlet, "Numerical investigation of the effect of non-isotherme sorption characteristics on hygrothermal behavior of two bio-based building walls," *Journal of Building Engineering*, vol. 7, pp. 263-272, 2016.

[14] E. Latif, R. Lawrence, A. Shea, and P. Walker, "An experimental investigation into the comparative hygrothermal performance of wall panels incorporating wood fibre, mineral wool and hemp-lime," *Energy and Buildings*, vol. 165, pp. 76-91, 2018.

[15] D. Lelievre, T. Colinart, and P. Glouannec, "Hygrothermal behavior of bio-based building materials including hysteresis effects: Experimental and numerical analyses," *Energy and Buildings*, vol. 84, pp. 617-627, 2014.

[16] M. Labat, M. Woloszyn, G. r. Garnier, and J. J. Roux, "Dynamic coupling between vapour and heat transfer in wall assemblies: Analysis of measurements achieved under real climate," *Building and Environment*, vol. 87, pp. 129-141, 2015.

[17] E. Latif, S. Tucker, M. A. Ciupala, D. C. Wijeyesekera, D. J. Newport, and M. Pruteanu, "Quasi steady state and dynamic hygrothermal performance of fibrous Hemp and Stone Wool insulations: Two innovative laboratory based investigations," *Building and Environment*, vol. 95, pp. 391-404, 2016.

[18] Z. e. C. PAVLÍK, Robert, "Hygrothermal performance study of an innovative interior thermal insulation system," *Applied Thermal Engineering*, vol. 29, pp. 1941-1946, 2009.

[19] T. Colinart, P. Glouannec, T. Pierre, P. Chauvelon, and A. Magueresse, "Experimental study on the hygrothermal behavior of a coated sprayed hemp concrete wall," *Buildings*, vol. 3, pp. 79-99, 2013.

[20] Y. Aït Oumeziane, S. Moissette, M. Bart, F. Collet, S. Pretot, and C. Lanos, "Influence of hysteresis on the transient hygrothermal response of a hemp concrete wall," *Journal of Building Performance Simulation*, vol. 10, pp. 256-271, 2017.

[21] M. Rahim, O. Douzane, A. T. Le, G. Promis, and T. Langlet, "Experimental investigation of hygrothermal behavior of two bio-based building envelopes," *Energy and Buildings*, vol. 139, pp. 608-615, 2017.

[22] O. Douzane, G. Promis, J.-M. Roucoult, A.-D. T. Le, and T. Langlet, "Hygrothermal performance of a straw bale building: In situ and laboratory investigations," *Journal of Building Engineering*, vol. 8, pp. 91-98, 2016.

[23] SOUTHERN, J. R. Summer condensation within dry lined solid walls. Building Services Engineering Research and Technology, 1986, vol. 7, p. 101-106.

[24] WALKER, Rosanne and PAVÍA, Sara. Thermal performance of a selection of insulation materials suitable for historic buildings. Building and environment, 2015, vol. 94, p. 155-165.

[25] SHEA, Andy, LAWRENCE, Mike, and WALKER, Pete. Hygrothermal performance of an experimental hemp–lime building. Construction and Building Materials, 2012, vol. 36, p. 270-275.

[26] C. Rode and K. Grau, "Moisture buffering and its consequence in whole building hygrothermal modeling," *Journal of Building physics*, vol. 31, pp. 333-360, 2008.

[27] G. Hedenblad, "Measurement of moisture in high performance concrete," presented at VTT SYMPOSIUM, 1997.

[28] M. Ferroukhi, K. Abahri, R. Belarbi, and K. Limam, "Integration of a hygrothermal transfer model for envelope in a building energy simulation model: experimental validation of a HAM-BES co-simulation approach," *Heat and Mass Transfer*, vol. 53, pp. 1851-1861, 2017.

[29] F. Collet and S. Pretot, "Experimental highlight of hygrothermal phenomena in hemp concrete wall," *Building and environment*, vol. 82, pp. 459-466, 2014.

[30] T. Colinart, D. Lelièvre, and P. Glouannec, "Experimental and numerical analysis of the transient hygrothermal behavior of multilayered hemp concrete wall," *Energy and Buildings*, vol. 112, pp. 1-11, 2016.